Pergamon

0301-9322(95)00087-9

Int. J. Multiphase Flow Vol. 22, No. 3, pp. 499–514, 1996

0301-9322/96 $15.00 + 0.00

EXPERIMENTAL STUDY OF THE EFFECT OF PIPE LENGTH AND PIPE-END GEOMETRY ON FLOODING

J. H. JEONG and H. C. NO

Department of Nuclear Engineering, Korea Advanced Institute of Science and Technology, 371-1 Ku Song Dong, Yu Sung Gu, Taejon 305-701, Korea

(Received 29 March 1995; in revised form 14 December 1995)

Abstract—The onset of flooding is thought to be highly sensitive to the end geometry of the test channel and its high sensitivity is an important cause of data scattering. In the present work, the effect of end geometry on flooding is experimentally investigated. Observation shows that flooding definition also causes the data scattering and that flooding should be classified into two modes according to the location where it occurs. With the sharp liquid entrance geometry, both entrance flooding and exit flooding are able to take place while only exit flooding does when entrance is smooth. In the range of low liquid flow rates, exit flooding always takes place and flooding gas velocities for the same exit geometry are nearly the same regardless of liquid entrance geometry. When air is injected into the test tube through a nozzle, even if the liquid exit is sharp, flooding gas velocities are nearly the same as those with smooth exit geometry. The present experiments show that the length effect is significantly affected by the pipe-end geometry. It is small in the range of low liquid flow rates but becomes significant as the liquid flow rate increases.

Key Words: flooding, length effect, pipe-end geometry

1. INTRODUCTION

Early notice upon flooding (CCFL) phenomena was taken in the 1930s by chemical engineers because a lot of chemical processes relied on the countercurrent gas–liquid flow to enhance both heat and mass transfer between two phases (English *et al.* 1963). Because of its importance in both the nuclear and process industries, various aspects of flooding phenomena have been studied extensively over the past four decades. A large number of models and experimental data have been produced as a result of numerous analytical and experimental works (Bankoff & Lee 1986, Tien & Liu 1979, Hewitt 1989). Most correlations and data on flooding were presented in terms of Wallis parameter (j_k^*) or Kutateladze number (Ku_k). Where,

$$j_k^* = j_k \sqrt{\frac{\rho_k}{gD(\rho_L - \rho_G)}}, \quad [1]$$

$$Ku_k^* = j_k \frac{\sqrt{\rho_k}}{(g\sigma(\rho_L - \rho_G))^{1/4}}. \quad [2]$$

In spite of such a large number of research, a satisfactory correlation applicable over a wide range of pipe geometry and fluid properties is still lacking. Wave instability is considered as a most plausible flooding mechanism. Zabaras and Dukler (1988) and Biage *et al.* (1989) investigated the characteristics of waves developed on the liquid film to supplement the flooding mechanism of wave instability. However, they did not care about the end geometry of the test section. Most investigators agree on the speculation that the onset of flooding is highly sensitive to the end geometry of the test channel and its high sensitivity is an important cause of data scattering. In order to show the effect of pipe end geometry qualitatively, Jeong and No (1994) analysed their flooding databank with entropy minimax principle which is useful to determine which data sets have similar trends. They showed that the flooding gas velocity generated with smooth liquid entrance and exit geometry is larger than that with a sharp geometry. Recently, Govan *et al.* (1991)

carried out a series of experiments to give direct comparison among flooding data which were obtained using porous wall, bell-mouth shape and square-edged water exit geometry. They also tried to explain the phenomena of liquid flow inside the test section before and after flooding occurs. As they did not change the entrance geometry but used only porous wall to introduce water into the test section, however, they could not observe how flooding phenomena are affected by the water entrance geometry. Also, they were not interested in the relation between the length effect and tube exit geometry. In this regard, the present work aims at investigation of the effects of tube-end geometry on flooding. Another point which have been controversial is the length effect on flooding. The effect of pipe length on flooding has been investigated by Hewitt *et al.* (1965), Grolmes *et al.* (1974), Hewitt (1977), Suzuki & Ueda (1977), Whalley & McQuillan (1985), Goven *et al.* (1991) and Lindarto *et al.* (1991). All the investigators used a porous wall in order to introduce liquid to the test pipe. Hewitt *et al.* (1965), Whalley & McQuillan (1985), Goven *et al.* (1991) and Lindarto *et al.* (1991) used the porous wall in order to remove the liquid film while the other investigators discharged the liquid film into the lower plenum. However, they reported contradictory results. Grolmes *et al.* (1974) and Hewitt (1977) reported that the length effect on flooding was negligible while the others reported that flooding gas velocities decreased as the length of the pipe between liquid entrance and exit was increased. In spite of their strictly opposite experimental results, there have been few works to find the cause of the contrary observations. In the present work, the length effect and the cause of the contrary observations are also investigated.

2. EXPERIMENTAL APPARATUS

An experimental loop was constructed to perform flooding experiments with various entrance and exit geometries and pipe lengths. Its schematic diagram is shown in figure 1. The loop consists of air flow meters, liquid flow meters, a liquid reservoir, a pump, a blower, a 40 cm i.d., 50 cm long upper plenum and a 40 cm i.d., 60 cm long lower plenum. Upper and lower plenums are interconnected by a test pipe. The apparatus is supported by a frame made of steel slotted angle. Air compressed by a 7 HP centrifugal blower is injected into the lower plenum via a control valve and air flow meters and allowed to flow upwards through the test pipe and goes to the atmosphere.

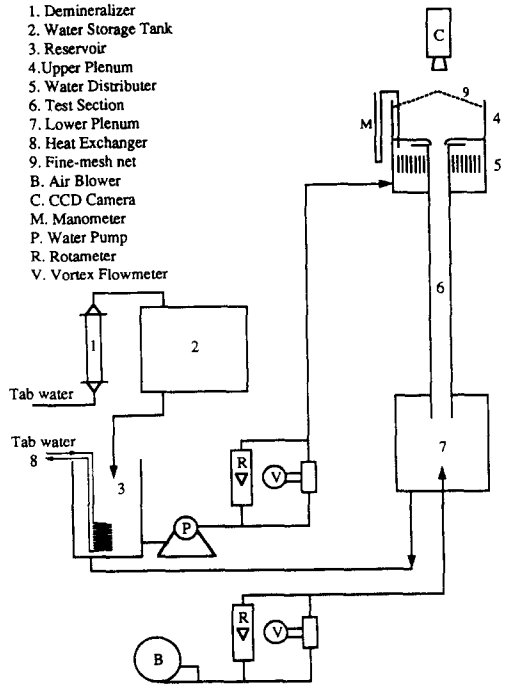

Figure 1. Schematic diagram of experimental loop.

Since the ions dissolved in tap water cause the drift of the water flow meters and make the material properties of tap water different from those of pure water, deionized water is used in this experiment. Ions dissolved in water are removed by ion-exchanger resin. The resins are contained in a fixed-bed ion-exchanger whose volume and length are 3 l and 1.2 m, respectively. Tap water is processed at the rate of 5 l/h and is accumulated in a reservoir. Part of water pumped from the reservoir goes to the upper plenum after passing through liquid flow-meters and the remainder flows back to the reservoir through a by-pass line. The water supplied to the bottom of the upper plenum flows upwards through a honeycomb-type flow distributor. The flow distributor minimizes azimuthal and radial variations of the water height in the upper plenum. It is made of 5 mm i.d., 8 cm long straws agglomerated around a small pipe. The water in the upper plenum overflows into the test pipe and flows downwards along the wall of the test pipe by gravity and goes back to the reservoir. Since the water is circulated in the closed test loop, sensible heat due to pump work is added to the water and, in turn, the water temperature is continuously increased during experiments if there is no effective heat sink. In order to remove the sensible heat and maintain the water temperature constant, the water contained in the reservoir is cooled by tap water flowing through a 5 mm i.d. copper pipe emerged in the reservoir during experiments. A fine-mesh net which covers the upper plenum separates entrained water. Entrained water trapped in the net flows back to the upper plenum.

Transparent acrylic resin pipes having 3 cm in inner diameter and 50, 100, 200 cm in lengths were used as test sections. In order to test the effects of end geometries on the flooding gas velocity, water inducers made of acrylic resin were installed at the pipe ends with rounded, protruded, and squared end geometries. Rounded inducer is made of acrylic resin block. Its surface changes smoothly from horizontal to vertical direction. The radius of curvature of the surface is 3 cm. It is installed in a manner that its end fits well with the inner surface of the test pipe. The protruded end geometry represents the protruded pipe whose end is straight flushed. The squared inducer represents the geometry that a horizontal plate is attached at the end of straight flushed pipe. These types of end geometry are the same as those adopted by Bharathan *et al.* (1979). In order to investigate the effects of air injection methods, two typical methods, sparger and nozzle, were used. The sparger located outside of the test pipe supply air to the lower plenum through 5 mm i.d. of holes which are uniformly spaced. The nozzle is a straight pipe having 10 mm i.d. The nozzle is installed so as that it is aligned with the tube axis and its end is inserted in the test pipe. The air is introduced into the test pipe directly through the nozzle.

The air flow rate is measured by two rotameters and a vortex flow-meter which have the operation ranges of 2–200 SCFH, 140–1200 SCFH, 480–4800 SCFH, respectively. The water flow rate is measured by two rotameters and a vortex flow-meter which have the operation ranges of 0.2–2.55 LPM, 0.2–2.5 GPM, and 1.5–20 GPM, respectively. Current signals coming from the two vortex flow-meters are read by the HP3457A digital multimeter, and the readings are transferred to a IBM-PC/AT and displayed on the monitor screen dynamically.

3. TEST CONDUCT

The flooding point can be reached either by setting the gas flow at a constant value and increasing the liquid flow or vice versa. Although a few works (Hewitt & Wallis 1963) employed the first method, Clift *et al.* (1966) reported that the above two methods produce identical results. In this work, the second method is employed. First of all, water flow supplied to the upper plenum is regulated to fix the flow rate at a predetermined value. Next, air is injected at the lowest attainable flow-rate into the lower plenum. When the flow condition reaches steady state, the air flow rate is increased a little and the test section is observed for about 10 min. A stepwise increase in the air flow rate is continued until the flooding is observed. The above procedure is repeated with a stepwise increase in the water flow rate. The flooding condition is determined by visual observation. The behavior of water in the upper plenum as well as of the water film in the test pipe is observed, because it is necessary to observe whether the highly agitating chaotic flow region propagated through all the test pipe and whether the entrance flooding takes place or not. The behavior of the water in the upper plenum can be observed by a mirror which is installed slanted above the upper plenum. These measurements are carried out with various end geometrics and pipe lengths.

An identifier is being assigned to the data set from each geometry type. Each identifier consists of 6 characters. The first and second characters represent liquid entrance and exit geometry, respectively. B, J, and K represent that the end geometry is rounded inducer, protruded pipe and squared inducer, respectively. O, W, and X represent the same types of end geometry as those of B, J, and K, respectively but have a different air injection mode; air for O, W, and X is supplied into the test section directly via a nozzle while it for B, J, and K is supplied through a sparger via the lower plenum. The third character and fourth through sixth characters represent diameter and length of the test section in cm, respectively.

Three kinds of errors are involved in measuring the flooding gas velocity in this experiment. They are an inherent error of the instrument, reading error, and systematic error which is introduced due to experimental procedure. Since the air flow rate is increased stepwisely until the flooding gas velocity is judged to be reached, there is a systematic error which is the difference between judged and actual flooding gas velocities. The flowmeters used in these experiments are accurate within $\pm 2\%$. If we assume that we can read the indicator within $\pm 5\%$ errors and that the systematic error is less than $\pm 10\%$ of the exact value, the maximum error for reading Q_k is

$$\Delta Q_k = (1.05 \times 1.02 \times 1.1 - 1)Q_k = 0.178Q_k. \quad [3]$$

When the inaccuracy of each instrument is known, the error bound of the computed result is estimated by the method of error propagation (Doebelin 1977). According to this method, the measurement error in terms of Wallis parameter is about 10%.

4. RESULTS AND DISCUSSION

Pipe end geometries will be frequently mentioned in the course of description of the experimental results and phenomena hereafter. Since flooding phenomena have been investigated in order to know whether the countercurrently flowing liquid can penetrate the flow path or not, the terms *entrance* and *exit* will be used to denote the water entrance and exit of the test section, respectively.

Earlier investigators presented many initiating events and models on flooding with various phenomenological definitions such as liquid drop entrainment, liquid flow reversal, zero liquid penetration, liquid bridge, chaotic flow pattern, and sudden change of gas pressure across the test section. These various definitions considerably influence the model description and yield systematic differences in the measurement of the flooding gas velocity. All these phenomena can be explained with a single event and its successive results. When liquid flows downwards, solitary waves are developed on the surface of the liquid film (Alekseenko *et al.* 1985, Dukler 1977). Above a certain gas flow rate, solitary waves grow abruptly. The abruptly grown solitary waves produce liquid entrainments and may block the gas flow path, so that it may result in a liquid bridge and a sudden increase in pressure difference across the test section. Under this situation a chaotic flow pattern is expected. In order to understand the effects of flooding definitions on the flooding data points reported by other investigators, three different gas velocities for a fixed water velocity were measured in this work.

4.1. Observation on rounded entrance case

In the cases that entrance is equipped with a rounded inducer, a smooth water film is developed over the inducer and on the inner surface of the test pipe. As the film flows downward along the pipe inner surface, waves are developed on the surface of the film even if there is no gas flow. When a gas flow rate exceeds a certain value, compared with ripples, a large-amplitude and large wavelength waves are observed. These large waves look like a semicircle and are separated about 10 cm in the vertical direction between each successive one. These are considered to be a type of roll waves. Their amplitudes grow to the maximum around the exit. When an air flow rate is increased to a certain value, one of them grows suddenly to hinder the gas flow and produce many entrainments. At this time, wavy countercurrent annular flow was transformed into a highly turbulent chaotic flow pattern. This transition phenomena is termed *exit perturbation* in this work. For sharp exit geometry such as protruded pipe and squared inducer, the chaotic flow region does not propagate upward but is limited only in a narrow region around the pipe exit and the smooth annular flow pattern is maintained in the other part of the test section. As the air flow rate is

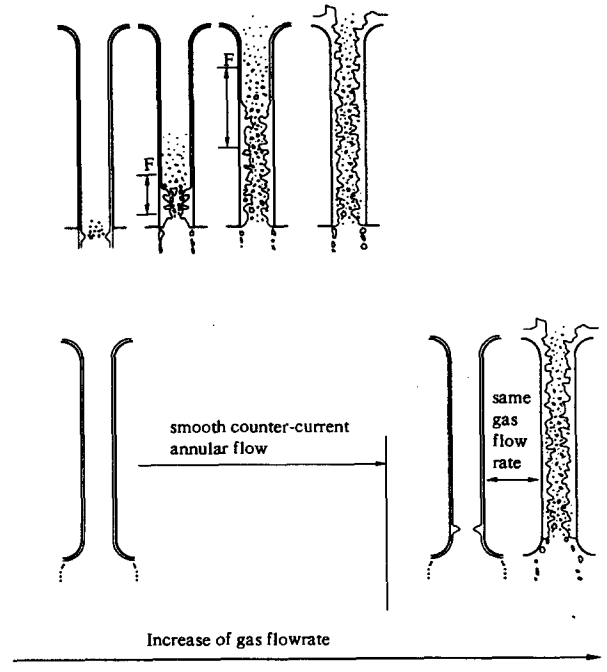

F : Fluctuation range of chaotic flow pattern region

Figure 2. Schematic diagram of flooding.

increased, the chaotic flow patten region is gradually propagated upwards with a large fluctuation of its region as shown in figure 2. These observations are a little different from those of Govan *et al.* (1991). They reported that, in case of sharp exit geometry, a churn-type flow (chaotic flow) suddenly rushes up the pipe at a certain air flow rate. Even though many drops are generated by the interaction between the two phases, most of them are deposited on the falling film and the surface of water contained in the upper plenum and flow downward again. Therefore, entrainment appears not to be a precursor of flooding but to be a product of flooding. In this range of air flow

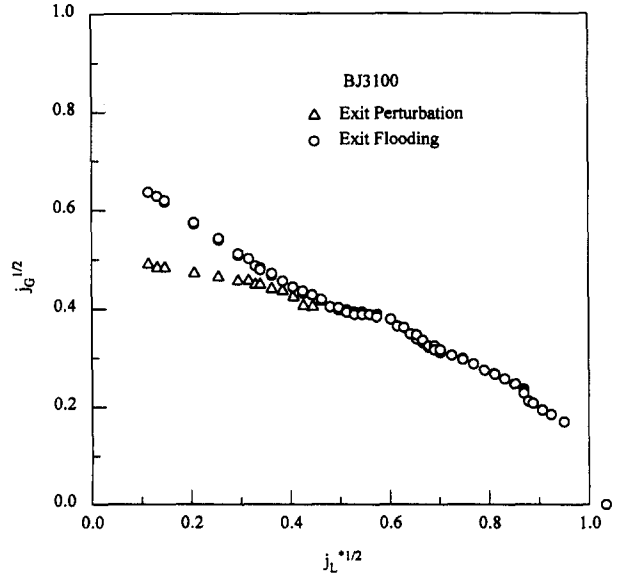

Figure 3. Measurements for the 3 cm i.d., 100 cm long test section with a rounded entrance and protruded exit.

rates, all the water supplied into the upper plenum can penetrate the test section. Even though the smooth countercurrent annular flow pattern is not preserved, therefore, this situation is not considered as a limiting condition in the viewpoint of engineering applications. With a larger increase in the air flow rate, the chaotic flow pattern region finally reaches the entrance and a part of the liquid feed is not able to penetrate the flow path and is accumulated in the upper plenum. This point should be considered as a limiting condition in the viewpoint of engineering applications because all the water supplied into the upper plenum can not flow downwards. This transition point is defined as *exit flooding* in this work. The term *exit* represents the fact that flooding is initiated around the water exit. Figure 3 shows the measurements for the 3 cm i.d., 100 cm long test section of which entrance and exit are equipped with a rounded inducer and a protruded pipe, respectively. When the chaotic flow pattern is developed initially around the exit and is propagated through the whole test section, they are called *exit perturbation* and *exit flooding*, respectively. The above descriptions are related to the flooding mechanism in a test section with a sharp exit.

When both ends are equipped with rounded inducers, a chaotic flow pattern region is propagated to the entrance as soon as it appears around the exit with no increase in air flow rate. In this case, gas velocities for *exit perturbation* are the same as those for *exit flooding*. And this transition takes place at very higher gas flowrates than those for the sharp exit cases, as shown in figure 2.

4.2. Observation on sharp entrance case

When water is supplied into the test section by overflowing from an upper plenum, water moves horizontally towards the center before it flow downwards along the inner surface of a vertical pipe. For the test section with sharp entrance the flow direction is abruptly changed from horizontal to vertical direction while it changes smoothly in the case that the test section is equipped with a round inducer. Because of its abrupt change of the flow direction, a wave-like non-uniform flow is developed at the entrance as shown in figure 4. In the test section with the sharp entrance, a different flooding mode is observed because the peak of the non-uniform flow can become unstable earlier than large waves developed on the surface of water film inside the test pipe.

In the low range of water flow rate, the sequence of events occurred in the test section with sharp entrance is somewhat similar to that with a rounded inducer. However, in the high range, the non-uniform flow becomes unstable while the waves developed on the water film inside the test pipe are stable with the same air flow rate. Then it is hard to preserve the non-uniform flow in a smooth counter-current annular flow pattern. A sequence of photographs taken by a digital high speed camera is shown in figure 5. It is an axial view of entrance, and shows the behavior of the non-uniform flow just when flooding occurs. The time interval between two consecutive frames except between (a) and (b) is 1/250 s. Frame (a) was taken 20/250 s earlier than frame (b). Waves are developed in the azimuthal direction on the peak of the non-uniform flow. This mechanism is named *entrance flooding* in this work because it is initiated by a loss of stability of the non-uniform flow developed at the entrance. Figure 6 shows the measurements for the 3 cm i.d., 100 cm long test section of which both ends are protruded pipes. In all the figures presented in this paper, entrance flooding and exit flooding are indicated by solid and open symbols, respectively. In the intermediate range between the above two ranges, $0.25 < j_L^{*1/2} < 0.5$, it is considered that the entrance flooding compete with the exit flooding. Although they compete with each other, this

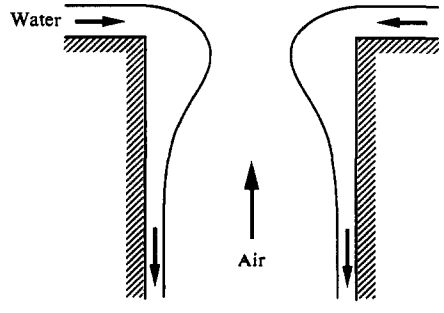

Figure 4. Schematic of non-uniform flow at the entrance.

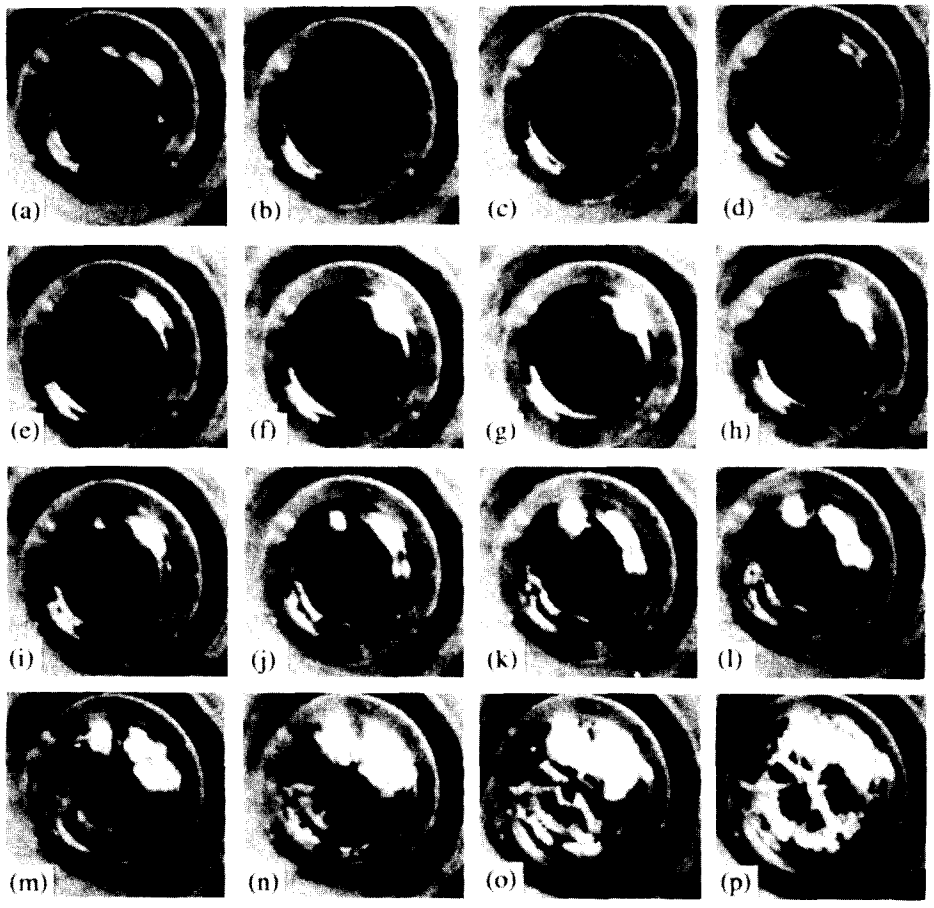

Figure 5. Sequential pictures of entrance flooding.

regime belongs to the entrance flooding because the entrance flooding occurs before the chaotic flow pattern initiated at the exit reaches the entrance.

There have been a few investigators who performed flooding experiments with protruded pipe entrance. Among them, Chung *et al.* (1980) and Kaminaga *et al.* (1991) reported the occurrence

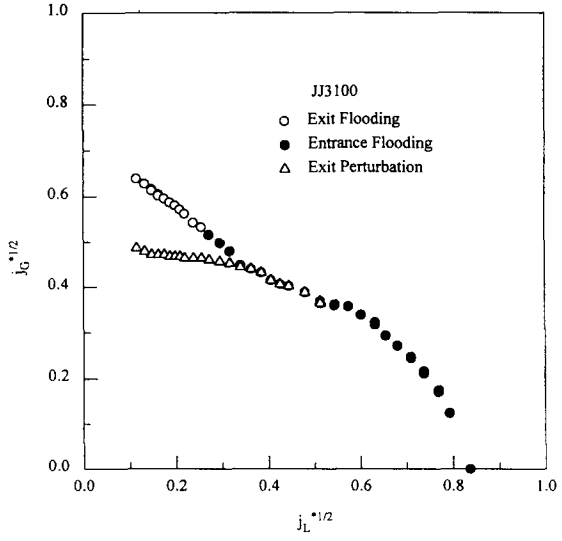

Figure 6. Measurements for the 3 cm i.d., 100 cm long test section with protruded entrance and exit.

of the entrance flooding mode. Chung *et al.* (1980) reported that when the protruded pipe entrance and nozzle air supply mode was used, flooding always takes place at the entrance without previous droplet entrainment and subsequent film agitation. However, Chung *et al.* (1980) did not make any distinction in their flooding data. They speculated that the cause of entrance flooding was the local thickening of the liquid film around the entrance. However, according to the observation of this experiment, entrance flooding was found to occur above a certain liquid flow rate. That is to say, when the water flow rate is small, the predominant flooding mode is not entrance flooding but exit flooding although the entrance geometry is sharp as shown in figure 6. It can be speculated that there are two reasons as the causes of the different observations between this experiment and that of Chung *et al.* The first one is the range of the water flow rate. Since Chung *et al.* performed the experiments above $Ku_L^{1/2} = 0.46$ (it corresponds to $j_L^{*1/2} = 0.25$ when the pipe inner diameter is 3.18 cm), it is probable that entrance flooding is dominant in his experiments. Another one is the non-symmetrical water supply. They said that additional calming device was used to make the water spilled into the pipe contact the pipe-wall uniformly. According to experiences, the careful design of a calming device is very important to suppress fluctuation and to ensure an even distribution of water around the periphery of the pipe. If there were fluctuations on the surface of the flow around entrance or if the flow was not symmetrical, entrance flooding might be promoted. Figure 5 shows that the instability of azimuthal directional waves developed on the peak of non-uniform flow is a more probable cause. Kaminaga *et al.* (1991) considered the instability of the wave-like non-uniform flow as the cause of entrance flooding. They got the wave number by applying their experimental data to the theoretical model which had been developed by Imura *et al.* (1977) on the basis of potential flow assumption. They considered the calculated wave number as the axial directional wave number of the non-uniform flow. That is because they did not observe the azimuthal directional waves developed on the non-uniform flow like as shown in figure 5. Considering the observation that the azimuthal directional waves more dynamically while the axial directional wavelike flow shape does not move in the axial direction, it is believed that the azimuthal directional wave number is more important than the axial directional one.

Void fraction is an important parameter affecting the flooding gas velocity. To measure the void fraction at the peak of non-uniform flow, the pictures of the non-uniform flows were taken by a digital camera attached above the test section. Void fractions were calculated by measuring the dimensions of video images. In order to find the interrelation, if any, between void fraction and the pipe diameter, four different pipe diameters were used: 2, 3, 4 and 5 cm. Figure 7 shows the interrelation between liquid fraction, ϵ_L, and $j_L^{*2/3}$. The liquid fraction is found to be able to be correlated linearly with $j_L^*2/3$ without dependency on the pipe diameter. A linear regression for all data shown in figure 7 gives two values, a constant term and the coefficient of the first order term.

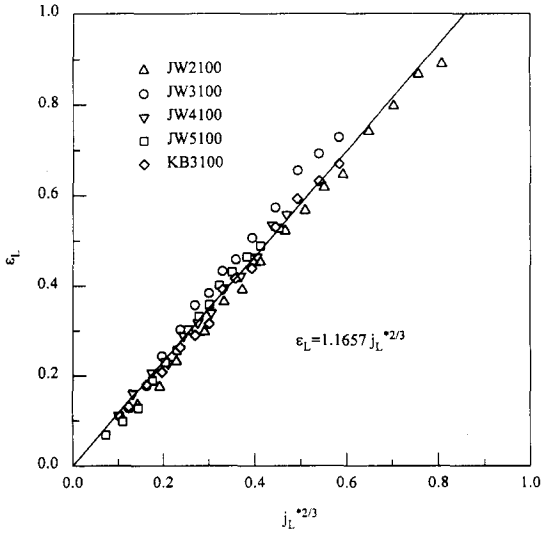

Figure 7. Entrance void fraction.

As the liquid fraction is zero when liquid flow rate is zero, however, the linear model for ϵ_L and $j_L^*2/3$ is chosen to have only the first order term. The best-fitting equation obtained by the method of least squares is as follows:

$$\epsilon_L = 1.166 j_L^{*2/3}. \quad [4]$$

Equation [4] is nearly the same result as Kaminaga *et al.* (1991)'s one of which proportional coefficient is 1.143.

4.3. Flooding definitions

The experimental definition on flooding appears to vary from one author to the other. Wallis (1961) took flooding data at the point where the liquid film became chaotic and Kaminaga *et al.* (1991) regarded the maximum gas flow rate at a certain liquid flow rate in a stable countercurrent flow condition as datum at the onset of flooding. The definition employed by the above two works is equivalent to *exit perturbation* named in this work. Hewitt & Wallis (1963) considered that flooding took place when the whole flow is disrupted and the liquid is expelled from the top of the pipe. This definition is equivalent to *exit flooding* named in this work. Celata *et al.* (1992) and Dukler & Smith (1979) took flooding data at the moment when the liquid falling film begins to be entrained by the upwards flowing gas. Bankoff & Lee (1986) considered that these differences do not seem to affect the flooding velocity substantially because they thought that flooding phenomenon develops rapidly and, as a result, the events described above take place nearly simultaneously. As can be seen in figures 3 and 6, however, an experiment carried out with sharp exit geometry can present two largely different flooding gas velocities according to whether investigators refer to *exit perturbation* or *exit flooding* as a flooding definition because there is a large discrepancy between the two gas velocities. The present data measured with squared entrance and protruded exit (KJ) geometry are compared with Kaminaga *et al.* (1991)'s data in figure 8. Kaminaga *et al.*'s data have been measured with the same geometric condition as that of the present data. Kaminaga *et al.*'s flooding data are closer to the exit perturbation data rather than the flooding data of the present experiments in the region of $j_L^{*1/2}$ less than 0.4 because Kaminaga *et al.*'s experimental definition on flooding is the same as that of the present exit perturbation. In the region of $j_L^{*1/2}$ greater than 0.4, the data points of the two data sets are nearly the same because of a small discrepancy between exit perturbation and exit flooding and the flooding mode is transferred to entrance flooding at which the two different definitions make little difference. Also in the case that both ends of the test pipe are equipped with rounded inducers, use of two different definitions makes no difference because gas velocities for *exit perturbation* and for *exit flooding* are the same. Therefore, Bankoff & Lee (1986)'s speculation is proper only for this case. From now on, only two

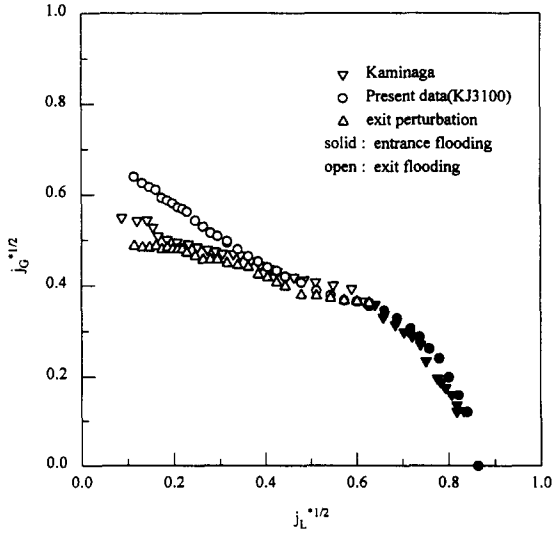

Figure 8. Comparison of experimental flooding definition.

types of flooding, *entrance flooding* and *exit flooding*, are considered as flooding modes and shall be presented in this paper because the *exit perturbation* is of no importance in the viewpoint of engineering applications.

4.4. *Effects of end geometry*

In order to investigate the effects of end geometries on flooding, experiments are performed with some types of end geometry. Figure 9 shows the flooding gas velocities measured with the 3 cm i.d., 1 m long test section of which entrance and exit geometries are rounded and rounded (BB), rounded and protruded pipe (BJ), protruded pipe and rounded (JB), and protruded pipe and protruded pipe (JJ). When the entrance has a protruded pipe (JB, JJ), both entrance flooding and exit flooding are able to take place depending on the water flow rate while only exit flooding does when entrance is equipped with a rounded inducer (BB, BJ). Flooding gas velocities measured in the test section of which both ends are equipped with rounded inducers are larger while those measured in the test section of which both ends have protruded pipes are smallest. This characteristic is consistent with the generally accepted idea concerning flooding gas velocities. Flooding points measured with JB geometry are close to those measured with BB geometry when water flow rates are small. At a certain value of the water flow rate, the flooding mode is changed from exit flooding to entrance flooding and the flooding gas velocities are abruptly decreased. The flooding points get closer to those measured with JJ geometry. It is noteworthy that flooding points do not jump discontinuously but are decreased continuously from those of BB to of JJ when the flooding mode is transferred from exit flooding to entrance flooding. According to this observation, it can be said that entrance flooding is a little affected by exit geometry. It is speculated that the effects of exit geometry are transmitted to the non-uniform flow developed at the entrance by virtue of entrainment. That is to say, liquid drops carried over by air flow give perturbations to the surface of the non-uniform flow when they are deposited on the surface. In such a condition for which larger amount of entrainment is generated, entrance flooding is able to occur at a lower gas velocity because the more the amount of entrainment is, the larger the perturbation is. Figure 9 shows the comparison between entrance flooding data measured with JB geometry and with JJ geometry. The second ones show lower $j_G^{*1/2}$ data points than the first ones do. It is because more entrainment is generated with JJ geometry due to sharp exit geometry. Data points of BJ geometry show a similar trend with those of BB geometry and are higher than those of JJ geometry.

When the water flow rate is small, the flooding gas velocities measured with BB and BJ geometry are nearly the same as those measured with JB and JJ geometry, respectively, while there is a large discrepancy between those measured with BB and JB geometry and with BJ and JJ geometry. When the water flow rate is large, the flooding gas velocities measured with JB and BJ geometry and with

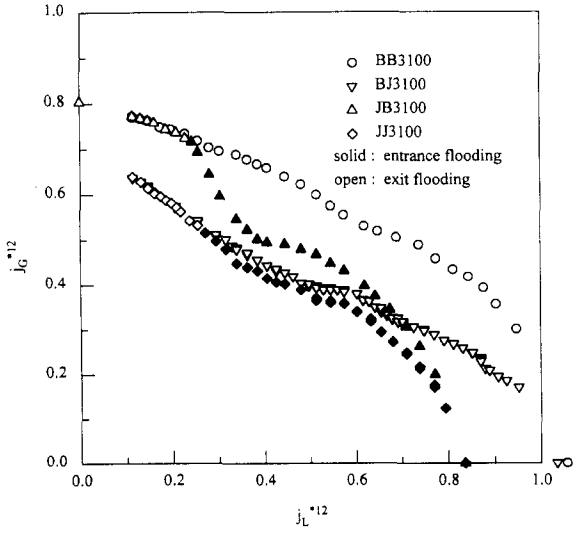

Figure 9. Effects of end geometries on flooding data.

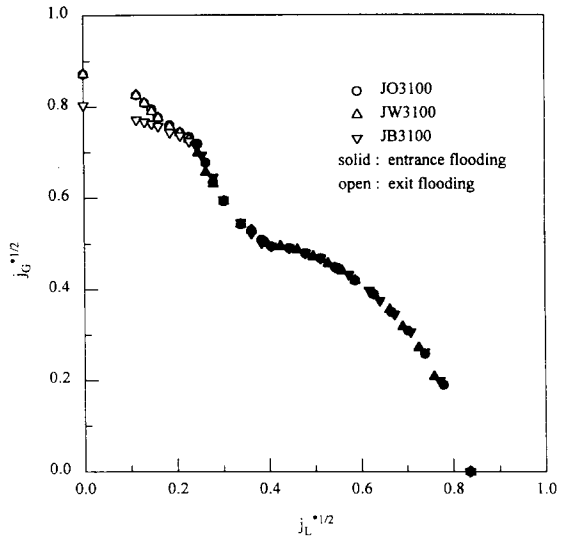

Figure 10. Effects of air injection mode.

JJ and BB geometry are getting closer to each other as the liquid flow rates increase while there is also a large discrepancy between those measured with JB, JJ geometry and with BJ, BB geometry. This experimental observation coincides with Jeong & No (1994)'s result which showed that flooding data points are classified according to exit geometry and entrance geometry when the liquid flow rate is small and large, respectively.

Figure 10 shows the effect of the air injection mode. In this figure the nozzle injection mode is compared with the sparger mode. Geometry identifiers JO and JW represent the conditions of which ends geometries are the same with JB, JJ geometries, respectively, and air is directly supplied into the test section via a nozzle. In the broad range of water flow rates except the narrow low range, flooding gas velocities measured with JO, JW geometries are nearly the same as those of JB geometry because interactions between air and falling water near the exit is weak. Although JW geometry has a sharp exit, a weak water–air interaction takes place like JB geometry having rounded exit because air is injected into the test section directly. This observation coincides with Jeong & No (1994)'s results: geometry having the nozzle injection mode belongs to the smooth exit group regardless of the geometry of the test section exit. In the narrow lowest range of water flow

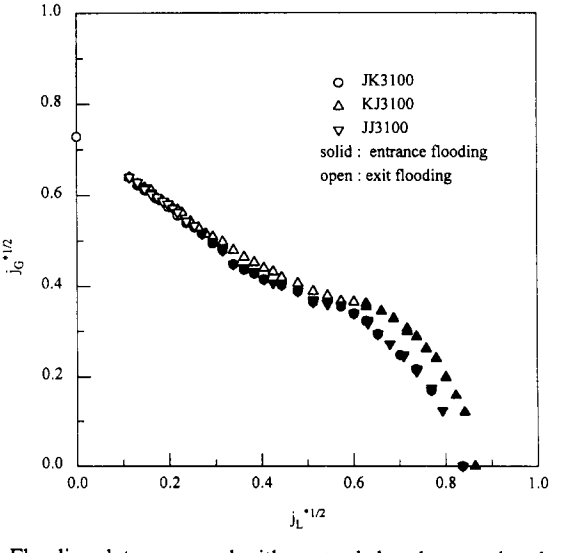

Figure 11. Flooding data measured with protruded and squared end geometries.

rates data from the nozzle injection mode data show higher gas velocities compared with those of JB geometry in which air is supplied via a sparger. The reason seems to be that, if the nozzle injection mode is used, there is a more or less air–water interaction because upward air flow first encounters the downward water flow at the upper location above the exit where waves are not grown to the maximum.

Figure 11 shows the comparison between the flooding data measured with protruded pipe geometry and with squared inducer geometry. As substantially negligible influence of the squared inducer can be observed, all subsequent analyses make no distinction between both results of protruded pipe and those of squared inducer.

4.5. Effects of test section length

In order to investigate the effect of pipe length, three different pipe lengths are used: 0.5, 1.0 and 2.0 m. The inner diameter of all the pipes used to investigate the length effect are 3 cm. Figures 12–15 show the length effect on flooding when BB, BJ, JB, and JJ geometries are used, respectively. These figures show that the pipe length effect on flooding can be differently observed according to the pipe end geometries. When BJ and JJ geometries which have sharp exit are used,

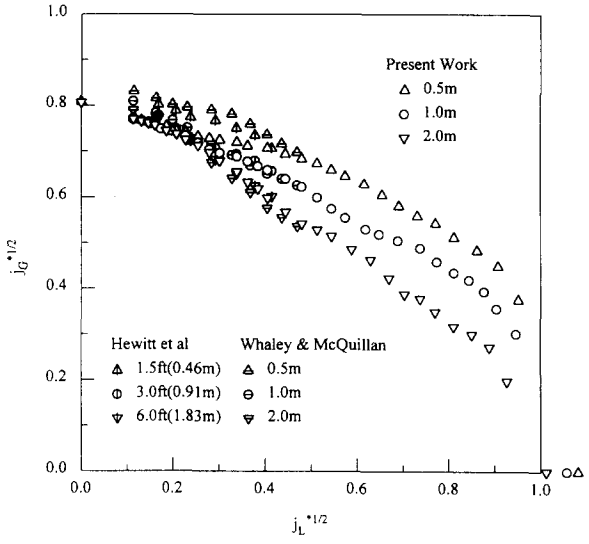

Figure 12. Flooding data for different pipe length with BB geometry.

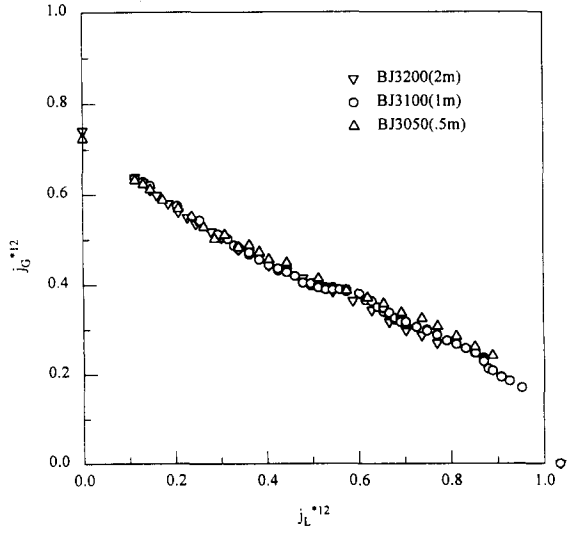

Figure 13. Flooding data for different pipe length with BJ geometry.

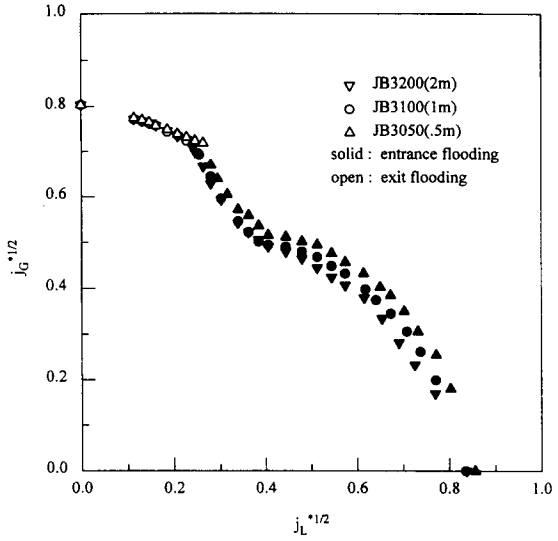

Figure 14. Flooding data for different pipe length with JB geometry.

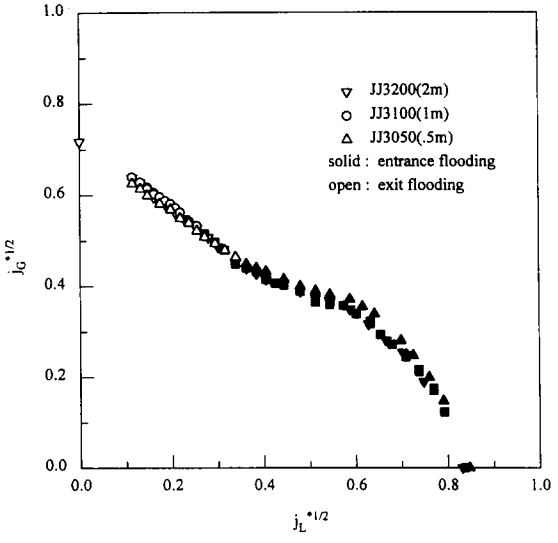

Figure 15. Flooding data for different pipe length with JJ geometry.

it seemed that the flooding gas velocity is not affected by the change of the test pipe length. When BB geometry is used, however, a significant length effect if observed. The flooding gas velocity is decreased with an increase in the pipe length. The pipe length effect on flooding is small for low liquid flow rates. However, it becomes larger as the liquid flow rate is increased. This trend is similar to the results observed by investigators who reported the existence of the length effect on flooding. When JB geometry is used, it seems that there is a little length effect. However, regarding the measurement errors, the length effect in JB geometry is thought to be negligible. These observations on the pipe length effect can be explained by the suggestion that flooding is caused by wave growth. Let us consider the case of BB geometry of which entrance and exit are smooth. Initial perturbations introduced at the entrance grow to large waves as they move downward. For given air and water flow rates the growth rate of the waves will be dependent only on the distance from the entrance of the pipe, so the wave height reaches a maximum just above the water exit and the maximum wave height will increase with the pipe length so far as the maximum wave height does not reach its saturation height. Flooding will occur only if the pipe is long enough to allow the waves to grow to the critical size in the test pipe. If the pipe is not long enough, air flow rates are needed to increase so that the wave height may become large enough to initiate flooding. Therefore,

flooding gas velocities decrease as the pipe length increases and the breaking of smooth counter-current annular flow is initiated in the vicinity of the exit as observed. In the case of JB geometry, entrance flooding takes place above a certain value of the water flow rate. Since entrance flooding is affected little by the flow condition in the test section below the entrance, it is speculated that flooding gas velocities are changed little with the change of pipe length. In the case of BJ geometry of which exit is sharp, the interaction between air and discharging water gives a large perturbation into the test section. When the exit is sharp, flooding takes place early and the length effect on flooding is not thought to be observed because flooding is initiated by strong interactions between falling liquid film and incoming gas near the exit and takes place with the lower gas velocity than needed to make the waves inside the test section grow to the critical size. Both rationales corresponding to the above two types of geometry, JB and BJ, are applied to JJ geometry for which no length effect is observed. The above rationales are confirmed by the previous investigators' work. In order to discharge falling water film, Hewitt *et al.* (1965), Suzuki & Ueda (1977), Whalley & McQuillan (1985) and Govan *et al.* (1991) employed smooth exit such as the bell shaped section or porous sinter section while Grolmes *et al.* (1974) and Hewitt (1977) employed sharp exit. The exit geometry employed by Hewitt (1977) was a diagonal cut at the bottom of the pipe. Therefore, Grolmes *et al.* (1974) and Hewitt (1977) were not able to observe the length effect while the others were able to do. There is a case by which the above statements seem not to be correct. Zabaras & Dukler (1988) used bell-mouth shaped exit geometry and said that the flooding curve was independent on the test section length while Suzuki & Ueda (1977) reported significant length effect with the same exit geometry. The reason is explained as follows: When flooding occurs in a vertical annular flow system, penetrating downward water flow rate is reduced stepwise. (Celata *et al.* 1991, reported hysteresis effect in flooding and showed that deflooding curve lies below the flooding curve.) That is, there can be two water flow rates with the same gas flow rate at the flooding point. Hewitt *et al.* (1965), Whally & McQuillan (1985), Suzuki & Ueda (1977) adopted the water feed flow rates just before flooding occurs while Zabaras & Dukler (1988) did downward penetration flow rates after flooding occurs to present their flooding data. It is certain that water film which flow downwards before occurrence of flooding, rather than penetrating downflow under flooding condition, controls when flooding occurs. Therefore, it is not thought to be good to adopt penetrating downflow rates to present flooding data. That is, Zabaras & Dukler (1988)'s report about the length effect should be excluded because their way of flooding data presentation is not proper. In addition, Govan *et al.* (1991) reported that the water downflow (penetration) rate beyond flooding is independent of the length of the falling-film region. The present results obtained with BB geometry are compared with other results in figure 12. For the sake of direct comparison, the results of the present work are compared with those obtained at nearly atmospheric pressure with nearly the same diameter as that used in this experiment. Hewitt *et al.* (1965) and Whalley & McQuillan (1985) used 1.25 in (3.17 cm) and 3.2 cm i.d. test sections, respectively. The figure shows that three different results are in good agreement, though the present results are somewhat lower than the other results in the lower liquid flow rate. The present results cover the much wider range of liquid flow rates.

5. CONCLUSIONS

Although various aspects of flooding phenomena have been studied since four decades ago, a satisfactory correlation has not appeared until now. Earlier works found that one of the most important factor introducing discrepancies between a correlation and an experimental data set is the end geometry of the test section. However, the effect of end-geometry on flooding was not so clear because there have not been so many works about the effect. Another obscure aspect of flooding phenomena was the effect of the test section length. In this regard, the present work focused on the effect of end-geometry on flooding phenomena. Flooding is found to be classified into entrance flooding and exit flooding according to the location where it initiates. The move of the location is due to entrance geometry. Observation shows that flooding definition also causes the data scattering. When exit geometry is sharp and liquid flow rate is low, there is a significant difference between the onset of flooding and the point where whole flow is disrupted and the liquid is expelled for the top of the pipe. It also shows that the cause of the contrary observation on the length effect is the pipe-end geometry. The length effect on flooding is significant only when the

entrance and exit geometry are smooth. Otherwise, the length effect is negligible. Considering the above observations, it can be said that the end geometry of the test section is able to affect the flooding definition and length effect as well as flooding data points.

REFERENCES

Alekseenko, S. V., Nakoryakov, V. Ye & Pokusaev, B. G. 1985 Wave formation on a vertical falling liquid film. *AIChE* **31,** 1446–1460.

Bankoff, S. G. & Lee, S. C. 1986 A Critical review of the flooding literature. In *Multiphase Science and Technology*, Vol. 2 (Edited by Hewitt, G. F. Delhaye, J. M. & Zuber, N.), pp. 95–180. Hemisphere Publishing, New York.

Bharathan, D., Wallis, G. B., Richter, H. J. 1979 Air–water countercurrent annular flow, EPRI, NP-1165.

Biage, M., Delhaye, J. M. & Vernier, Ph. 1989 The flooding transition: A detailed experimental investigation of the liquid film flow before the flooding point. *ANS Proceedings*, National Heat Transfer Conference, pp. 53–60.

Celata G. P., Cumo, M., Farello, G. E. & Setaro, T. 1991 Hyteresis effect in flooding. *Int. J. Multiphase Flow* **17,** 283–289.

Celata, G. P., Cumo, M. & Setaro, T. 1992 A data set of flooding in circular tubes. *Experimental Thermal and Fluid Science*, Vol. 5, 437–447.

Chung, K. S., Liu, C. P. & Tien, C. L. 1980 Flooding in two-phase counter-current flow-II; Experimental investigation. *Physicochem. Hydr. J.* **1,** 209–220.

Clift, R., Pritchard, C. L. & Nedderman, R. M. 1966 The effect of viscosity on the flooding conditions in wetted wall columns. *Chem. Eng. Sci.* **21,** 87–95.

Doebelin, E. O. 1977 *Measurement Systems: Application and Design*, 4th edition, pp. 58–60. McGraw-Hill, New York.

Dukler, A. E. 1977 The role of waves in two phase flow: some new understandings. *Chem. Eng. Educat.* 108–117.

Dukler, A. E. & Smith, L. 1979 Two-Phase Interactions in Countercurrent Flow: Studies of the Flooding Mechansim, USNRC, NUREG/CR-0617.

English, K. G., Jones, W. T., Spillers, R. C. & Orr, V. 1963 Flooding in a vertical updraft partial condenser. *Chem. Eng. Prog.* **59**(7), 51–54.

Goven, A. H., Hewitt, G. F., Richter, H. J. & Scott, A. 1991 Flooding and churn flow in vertical pipes. *Int. J. Multiphase Flow* **17,** 27–44.

Grolmes, M. A., Lambert, G. A. & Fauske, H. K. 1974 Flooding in vertical tubes. *Ins. Chem. Engr. Symp. Ser.* **38** (multiphase flow system).

Hewitt, G. F. 1977 Influence of end conditions, tube inclination and physical properties on flooding in gas-liquid flows, HTFS-RS222, UKAEA, Harwell, England.

Hewitt, G. F. 1989 Countercurrent two-phase flow. *Proc. NURETH-4* (4th Int. Top. Mtg on Nuclear Reaction Thermal Hydraulics), pp. 1129–1144.

Hewitt, G. F., Lacey, P. M. C. & Nicholls, B. 1965 Transitions in film flow in a vertical flow, AERE-R4614, UKAEA, Harwell, England.

Hewitt, G. F. & Wallis, G. B. 1963 Flooding and association phenomena in falling film flow in a tube, AERE-R4022, UKAEA, Harwell, England.

Imura, H., Kusuda, H. & Funatsu, S. 1977 Flooding velocity in a counter-current annular two-phase flow. *Chem. Eng. Sci.* **32,** 79–87.

Jeong, J. H. & No, H. C. 1994 Classification of flooding data according to type of tube-end geometry. *Nuclear Engineering and Design*, **148,** 109–117.

Kaminaga, F., Okamoto, Y. & Shibata, Y. 1991 Evaluation of entrance geometry effect on flooding. *1st JSME/ASME Joint Int. Conf. on Nucl. Eng.*, Tokyo, pp. 95–100.

Lindarto, Lusseyran, F. & Cognet, G. 1991 Investigation of the flooding of a falling liquid film: flow characteristic and length effect. *Proc. Int. Conf. on Multiphase Flows '91*, Tsukuba, Japan, pp. 123–126.

Suzuki, S. & Ueda, T. 1977 Behaviour of liquid films and flooding in counter-current two-phase flow. Part 1: flow in circular tubes. *Int. J. Multiphase Flow* **3,** 517–532.

Tien, C. L. & Liu, C. P. 1979 Survey on vertical two-phase counter-current flooding, EPRI, NP-984.

Wallis, G. B. 1961 Flooding velocities for air and water in vertical tubes, AAEW-R123, UKAEA, Harwell, England.

Whalley, P. B. & McQuillan, K. W. 1985 Flooding in two-phase flow: the effect of tube length and artificial wave injection. *Physicochem. Hydr. J.* **6,** 3–21.

Zabaras, C. J. & Dukler, A. E. 1988 Countercurrent gas–liquid annular flow, including the flooding state. *AIChE* **34,** 389–396.